Search for sidereal modulation of the arrival directions of events recorded at the Pierre Auger Observatory

R.Bonino*, for The Pierre Auger Collaboration†

*Istituto di Fisica dello Spazio Interplanetario (INAF), Università di Torino and Sezione INFN Torino, Italy
†Observatorio Pierre Auger, Av. San Martín Norte 304, (5613) Malargüe, Mendoza, Argentina

***Abstract*. Using data collected by the Pierre Auger Observatory from 1 January 2004 until 31 March 2009, we search for large scale anisotropies in different energy windows above $2 \cdot 10^{17}$ eV. A Fourier analysis shows the presence of a $\sim 3\%$ modulation at the solar frequency, arising from modulations of the array exposure and weather effects on the showers. We study the sidereal anisotropies using a Rayleigh method which accounts for these effects, and the East-West differential method which is largely independent of them. No significant anisotropies are observed, resulting in bounds on the first harmonic amplitude at the 1% level at EeV energies.**

***Keywords*: large scale anisotropy Auger**

I. Introduction

The large scale anisotropy, and in particular its dependence on primary energy, represents one of the main tools for discerning between a galactic or an extragalactic origin of UHECRs and for understanding their mechanisms of propagation. The transition from a galactic to an extragalactic origin should in fact induce a significant change in the CR large scale angular distribution, giving precious hints on their nature and on the magnetic fields that modify their trajectories.

Different theoretical models predict the transition to occur at different energies and consequently lead to dissimilar predictions for the shape and the amplitude of the corresponding anisotropy. A measure of the anisotropy or the eventual bounds on it are thus relevant to constrain different models for the CR origin.

II. Data Analysis and results

The statistics accumulated so far by the Pierre Auger Observatory allows us to perform large scale analyses with a sensitivity that is already at the percent level. For this analysis we used data recorded from 1 January 2004 to 31 March 2009, removing the periods of unstable data acquisition ($\sim 3\%$ of the whole data set).

Searching for %-level large-scale patterns requires control of the sky exposure of the detector and of various acceptance effects, such as detector instabilities and weather modulations. The main effects are expected to appear at the solar frequency but may also be non-negligible at other frequencies. In particular, the combination of diurnal and yearly modulations of the acceptance may generate a spurious variation with similar amplitudes at both the sidereal and anti-sidereal frequencies [1]. The Fourier transform of the arrival times of the events is thus an ideal tool to analyse their frequency patterns and in particular the sidereal, solar and anti-sidereal modulations [2]. The resolution of this analysis is of the order of $1/T$, where T is the exposure time. Therefore, if data are acquired over a few years, even with variable detector conditions, the resolution is sufficient to resolve the sidereal and the diurnal frequencies. For each frequency the associated Fourier amplitude is calculated using the distribution of the times t_i of the events modified such that any sidereal modulation of $\tilde{t_i}$ is equal to the modulation of the event rate in Right Ascension:

$$\tilde{t_i} = t_i + \alpha_i - \alpha_i^0, \quad (1)$$

where α_i is the RA of the event and α_i^0 is the local sidereal time corresponding to UTC time t_i.

We show in Fig.1 the results of such analysis using the whole data set. The amplitude at the solar frequency largely stands out from the noise, whereas the amplitudes at all other frequencies stand at the level of the average noise (estimated to be 0.33% using data at all frequencies except for the solar band). In particular, the amplitudes at the sidereal and at the anti-sidereal frequencies are at a similar level. If a genuine large-scale pattern were present above the noise level, the amplitude at the sidereal frequency would clearly stand out the anti-sidereal one.

We repeated the same analysis for several energy ranges. The results are displayed in Tab.I, where the sidereal amplitudes (r_{sid}) are compared to the anti-sidereal ones (r_{a-sid}). It can be seen that there is no significant signal at the sidereal frequency within the available statistics.

TABLE I
Sidereal amplitudes (r_{sid}) compared to the anti-sidereal ones (r_{a-sid}) in 6 energy ranges. Also indicated are the typical statistical fluctuations through the average noise and its RMS.

Energy Range [EeV]	r_{sid} [%]	r_{a-sid} [%]	Average Noise [%]	σ_r [%]
0.2 - 0.5	0.66	0.61	0.41	0.22
0.5 - 1	0.44	0.52	0.36	0.20
1 - 2	1.08	0.82	0.52	0.28
2 - 4	1.37	1.36	0.88	0.43
4 - 8	1.26	0.84	1.68	0.86
>8	5.70	3.27	2.59	1.42

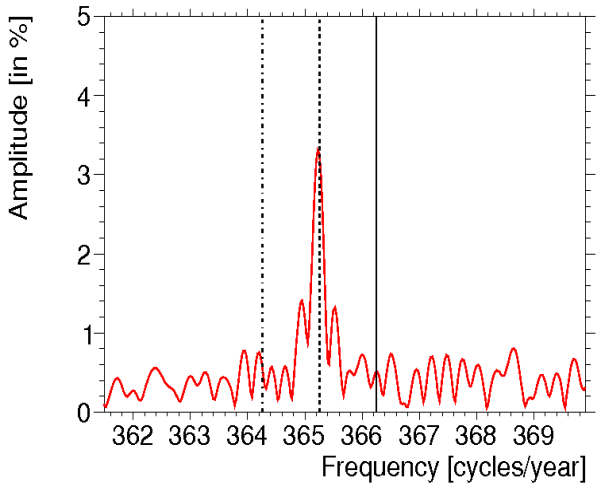

Fig. 1. Amplitude of the first harmonic as a function of the frequency, applying the Fourier time analysis on the whole data set. From left to right, the anti-sidereal and the solar frequencies are indicated by the *dotted vertical lines*, whereas the sidereal frequency is represented by the *continuous line*.

The variations due to the non-uniform detector on-times can be taken into account using a generalised Rayleigh analysis [3]. This method corrects for the effects of a non-uniform acceptance in right ascension by weighting each event with a factor ω_i inversely proportional to the relative exposure of the region of the sky observed at the arrival time of the event (α_{di} is the right ascension of the zenith of the detector at the time the event i is detected) [4]. These factors are obtained from the detailed information about the individual detector stations on-times. Computing the coefficients:

$$A = \frac{2}{\Omega}\sum_i \omega_i(\alpha_{di})\cos\alpha_i \qquad (2)$$

$$B = \frac{2}{\Omega}\sum_i \omega_i(\alpha_{di})\sin\alpha_i \qquad (3)$$

where $\Omega = \sum_i \omega_i(\alpha_{di})$, the Rayleigh amplitude and phase are obtained through:

$$r = \sqrt{A^2+B^2} \text{ and } \phi = \text{atan}\frac{B}{A} \qquad (4)$$

In this case the deviations from a uniform exposure are small, so the probability that an amplitude larger or equal to r arises from an isotropic distribution may be estimated with the standard expression $P = \exp(-k_0)$, where $k_0 = r^2N/4$ (being N the total number of events). In addition, we account for atmospheric effects, such as changes in the air density and pressure, in the energy estimation of each event [5]. This is the dominant weather effect above $\sim$ 1 EeV, while below that energy the weather effects also start to affect the trigger efficiency in a significant way. Hence, with this method we present results only above 1 EeV.

After applying such corrections all the spurious modulations are removed. For instance, in the energy interval $1-2$ EeV a first harmonic in solar time of 3.33% (corresponding to a chance probability $P \sim 10^{-20}$) is reduced to 0.88% ($P \sim 2\%$) after all the corrections. The corresponding first harmonics in sidereal and anti-sidereal time are of the same order, being respectively 0.90% and 0.71%, with a probability to result from a fluctuation of an isotropic distribution of $\sim 2\%$ and $\sim 8\%$.

An alternative method, which is largely independent of possible systematic effects, is the differential East-West method [6], which exploits the differences in the number of counts between the eastward and the westward arrival directions at a given time. Since the instantaneous eastward and westward acceptances are equal and the two sectors are equally affected by the instabilities of the apparatus, by making the difference in the East and West counts, this method allows us to remove direction-independent phenomena, such as atmospheric and acceptance effects, without applying any correction. The difference in the number of counts $E(t) - W(t)$ is related to the physical CR intensity $I(t)$ by $\mathrm{d}I/\mathrm{d}t = (E(t) - W(t))/\delta t$. The first harmonic analysis of $I(t)$, whose amplitude and phase are (r_I,ϕ_I), can be derived from the first harmonic analysis of $E(t) - W(t)$, of amplitude and phase (r_D,ϕ_D):

$$r_I = \frac{1}{\sin\delta t}\frac{n_{int}}{N} r_D \text{ and } \phi_I = \phi_D + \frac{\pi}{2} \qquad (5)$$

where N is the total number of events, n_{int} is the number of intervals of sidereal time used to compute the first harmonic amplitude of $E(t) - W(t)$ and δt is the average hour angle between the vertical and the events from sector E (or W). The probability that an amplitude equal or larger than r arises from an isotropic distribution is $P = \exp(-r^2 N \sin^2\delta t/4)$.

Since this method is largely independent of spurious time variations, the analysis can be performed also on the whole data set (median energy $\sim 6 \cdot 10^{17}$ eV), even below the energy threshold for full efficiency. For the complete data set the amplitudes in solar and anti-sidereal time are respectively 0.29% ($P \sim 55\%$) and 0.24% ($P \sim 66\%$), showing that any spurious modulation has been removed (the amplitude in solar time with the standard Rayleigh analysis, without corrections, is 3.98%). The corresponding amplitude in sidereal time is $r = 0.48\%$, the probability for it to result from a fluctuation of an isotropic distribution is $\sim 20\%$ (see the first line of Tab.II).

In Fig.2 the results of the E-W and the Rayleigh analyses on all the events above increasing energy thresholds are shown. No significant modulation in sidereal time is detected throughout the scan. The two methods are complementary: while the Rayleigh analysis can only be reliably used above 1 EeV, the East-West analysis can be safely applied even below 1 EeV but it is affected by larger statistical uncertainties.

For completeness and because the points in Fig.2 are correlated, we repeated the two analyses in energy

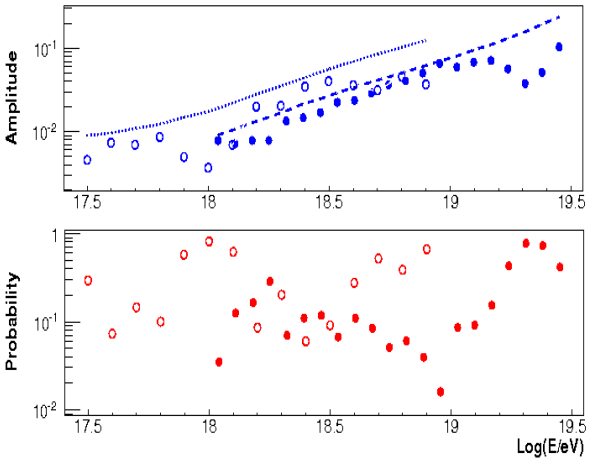

Fig. 2. Rayleigh amplitude (top) and probability for the amplitude to result from fluctuations of an isotropic background (bottom) as a function of increasing energy thresholds, obtained with both the generalised Rayleigh analysis, after correcting for non-constant acceptance and weather effects, (*filled circles*) and the East-West method (*empty circles*). The *dotted lines* indicate the 99% c.l. upper bound on the amplitudes that could result from fluctuations of an isotropic distribution.

bins of 0.1 Log(E). The results are shown in Fig.3 and provide a further evidence about the lack of significant modulations in sidereal time.

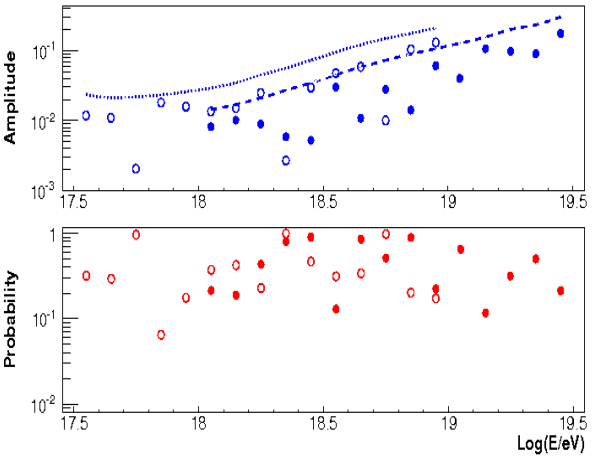

Fig. 3. The same as Fig.2 but here it is displayed for energy bins (instead of energy thresholds).

The statistics for some points of Fig.3 are obviously very low. Therefore we matched some of those energy intervals and repeated a first harmonic analysis using the two approaches. The results are collected in Tab.II. No significant departure from isotropy is observed with both methods. Having proved that both analyses account for the systematic effects, upper limits at 99% c.l. can thus be derived using only the statistical uncertainties. Such upper bounds, reported in the last column of Tab.II, have been calculated according to the distribution drawn from a population characterised by an anisotropy of unknown amplitude, as derived by J. Linsley in his 3^{rd} alternative [3].

III. Discussion

Studying large scale anisotropies as a function of energy may give a handle to study the galactic/extragalactic transition. We show in Fig.4 the upper limits obtained in this study, together with some predictions for the anisotropies arising from both galactic and extra-galactic models.

If the transition occurs at the ankle energy [7], cosmic rays at 10^{18} eV are predominantly galactic and their escape from the galaxy by diffusion and drift motions could induce a modulation at the percent level at EeV energies. The exact value strongly depends on specific models: Ptuskin et al. [8], considering different orientations of the local magnetic field and different positions of the observer, predict anisotropy amplitudes ranging from 10^{-6} up to 10^{-2}. We show in Fig. 4 the models discussed by Candia et al. [9], in which the predictions for the anisotropies up to EeV energies arising from the diffusion in the Galaxy are obtained. As these predictions depend on the assumed galactic magnetic field model as well as on the source distribution, two illustrative examples are shown. The bounds obtained here already exclude the predictions from the particular model with an antisymmetric halo magnetic field (A) and are starting to become sensitive to the predictions of the model with a symmetric field (S).

On the other hand, a second possible scenario considers the transition taking place at lower energies, i.e. around the so-called "second knee", at $\sim 5 \cdot 10^{17}$ eV [10]. In this case, at 10^{18} eV cosmic rays are dominantly of extra-galactic origin and their large scale distribution could be influenced by the relative motion of the observer with respect to the frame of the sources. For instance, if the frame in which the CR distribution is isotropic coincides with the CMB rest frame, the resulting anisotropy due to the Compton-Getting effect (*C-G Xgal* in Fig. 4) would be about 0.6% with a phase $\alpha \simeq 168^{\circ}$ [11]. This amplitude is very close to the upper limits set in this analysis (the statistics required to become sensitive to such amplitude at 99% c.l. is ~ 3 times the present statistics).

In the same figure we also display previous results from KASCADE, KASCADE-Grande and AGASA. A proper comparison of the results from different observatories should take into account the particular sky coverage of each experiment. All the anisotropy amplitudes have thus been divided by the mean value of the cosine of the declination of the observed sky, giving a direct measurement of the component of the dipole in the equatorial plane. The results presented here do not confirm the $\sim 4\%$ anisotropy reported by AGASA in the $1-2$ EeV energy bin [12] (however a proper comparison should take into account the peculiarities of the two experiments).

TABLE II
RESULTS OF THE TWO ANALYSES IN DIFFERENT ENERGY RANGES (THE EVENTS IN THE DIFFERENT ENERGY INTERVALS ARE SLIGHTLY DIFFERENT BETWEEN THE TWO METHODS BECAUSE THE RAYLEIGH ANALYSIS, UNLIKE THE EAST-WEST METHOD, CORRECTS THE ENERGY OF THE EVENTS FOR THE WEATHER EFFECTS). THE STATISTICAL UNCERTAINTIES ARE CHARACTERISED BY THE QUANTITIES $s_R = \sqrt{2/N}$ AND $s_{EW} = \sqrt{2/N}/\sin\delta t$. RAYLEIGH PROBABILITIES AND 99%C.L. UPPER LIMITS ARE ALSO GIVEN. SINCE ALL THE MEASURED AMPLITUDES ARE COMPATIBLE WITH BACKGROUND, THE PHASES ARE NOT SIGNIFICANT AND ARE NOT REPORTED HERE.

	Rayleigh analysis			**E-W method**			**upper limits**
Energy range [EeV]	r [%]	s_R [%]	P [%]	r [%]	s_{EW} [%]	P [%]	$r_{99\%}$ [%]
all energies				0.48	0.27	19.5	1.05
0.2 - 0.5				0.25	0.43	84.2	1.19
0.5 - 1				1.08	0.44	4.8	2.03
1 - 2	0.90	0.32	1.8	0.77	0.65	49.9	1.59
2 - 4	0.79	0.64	45.8	1.65	1.33	46.3	2.12
4 - 8	0.71	1.33	86.6	5.05	2.73	18.0	3.66
>8	5.36	2.05	3.3	2.76	4.08	79.5	9.79

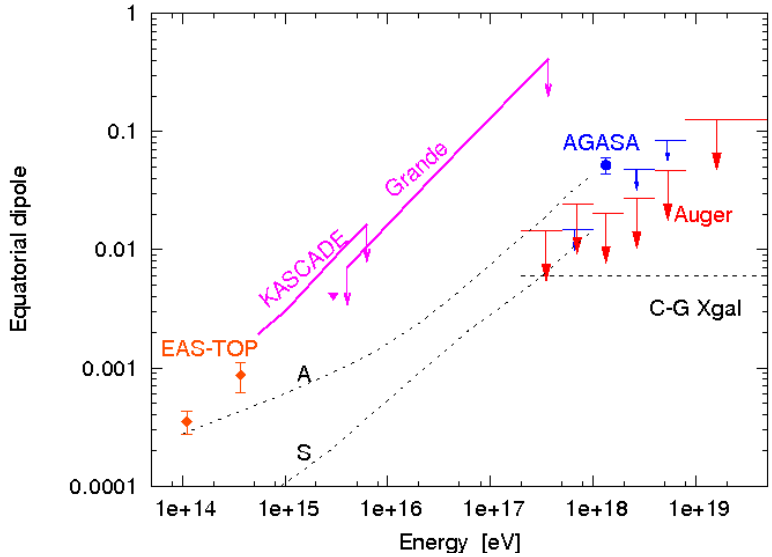

Fig. 4. Upper limits on the anisotropy amplitude as a function of energy from this analysis. Results from EAS-TOP, AGASA and KASCADE/Grande experiments are displayed too. Also shown are the predictions from two different galactic magnetic field models with different symmetries (A and S) and the expectations from the Compton-Getting effect for an extra-galactic component isotropic in the CMB rest frame (*C-G Xgal*).

IV. CONCLUSIONS

We have searched for large scale patterns in the arrival directions of events recorded at the Pierre Auger Observatory using two complementary analyses.

We have set 99% c.l. upper limits at the percent level at EeV energies, constraining some theoretical models. In particular, we can already exclude all those models that predict anisotropy amplitudes greater than $\sim 2\%$ below 4 EeV. Further statistics will obviously be useful, and the sensitivity will be improved in the coming years using data from the Pierre Auger Observatory.

Finally we do not confirm the 4% modulation detected by AGASA at 4 s.d. between 1 and 2 EeV.

REFERENCES

[1] F.J.M.Farley and J.R.Storey, *Proc. Phys. Soc. A*, 67:996, 1954.
[2] P.Billoir and A.Letessier-Selvon, *Astropart. Phys.*, 29:14-19, 2008.
[3] J.Linsley, *Phys. Rev. Lett.*, 34:1530-1533, 1975.
[4] S.Mollerach and E.Roulet, *JCAP*, 0508:004, 2005.
[5] Benjamin Rouillé d'Orfeuil [The Pierre Auger Collaboration], *these proceedings*, 2009.
[6] EAS-TOP Collaboration, *30th ICRC Merida*, 4:51-54, 2007.
[7] J.Linsley, *8th ICRC Jaipur*, 4:77-99, 1963.
[8] V.S.Ptuskin et al., *Astron. and Astrophys.*, 268:726, 1993.
[9] J.Candia et al., *J. Cosmol. Astropart. Phys.*, 05:003, 2003.
[10] V.Berezinsky et al., *Astron. and Astrophys.*, 74:043005, 2006.
[11] D.J.Schwarz et al., *Phys. Rev. Letters*, 93:221301, 2004.
[12] N.Hayashida et al., *Astropart. Phys.*, 10:303-311, 1999.